Central European Journal of Energetic Materials
ISSN 1733-7178; e-ISSN 2353-1843
Copyright © 2016 Institute of Industrial Organic Chemistry, Poland

Cent. Eur. J. Energ. Mater., 2016, *13*(3), 567-578; DOI: 10.22211/cejem/65014

The Preparation of NC Microspheres and BuNENA Modified NC Microspheres by the Breath Figures Method

Liming HE, [1,2*] Wei HE, [2] Yunjun LUO [1**]

[1] *School of Materials Science and Engineering, Beijing Institute of Technology, Beijing, China*
[2] *School of Chemical Engineering and Environment, North University of China, Taiyuan, China*
E-mails: [*]heliming@nuc.edu.cn; [**]yjluo@bit.edu.cn

Abstract: The 'breath figures' method was used to prepare nitrocellulose (NC) microspheres and N-butyl-N-(2-nitroxyethyl)nitramine (BuNENA) modified NC microspheres (BMNM). By using acetone as the solvent and non-solvent n-hexane as the atmosphere, NC microspheres and BMNM were obtained. The matching of solvents and non-solvents was the key factor influencing the final morphology. TG and DSC were employed to study the thermal decomposition characteristics of BMNM. The results suggested that there were two distinct stages of thermal mass loss from the BMNM: the first was the mass loss associated with partial volatilisation of BuNENA, and its activation energy was 68.54 kJ/mol. The second mass loss was the thermal decomposition of NC and residual BuNENA with a high activation energy (249.53 kJ/mol, calculated by the Kissinger method). According to the thermal decomposition kinetics model, the optimal kinetics model of BMNM was B1-A2. The addition of BuNENA did not influence the thermal decomposition of NC.

Keywords: 'breath figures' method, thermal decomposition, NC microspheres, BuNENA modified NC microspheres

1 Introduction

Cross-linked modified double-base (XLDB) propellants are regarded as important materials: the introduction of insensitive energetic plasticisers into XLDB propellants, replacing nitroglycerine (NG), is an effective way of achieving high-energy and insensitivity. Insensitive energetic plasticisers with good overall performance include: trimethylolethane trinitrate (TMETN), 1,2,4-butanetriol

trinitrate (BTTN), 1,5-diazido-3-nitrazapentane (DANPE or DIANP), bis(2,2-dinitropropyl)acetal/bis(2,2-dinitropropyl)formal (BDNPA/F), N-butyl-N-(2-nitroxyethyl)nitramine (BuNENA), *etc*. [1]. BuNENA has been used for its excellent overall performance [2-4]. BuNENA, as an insensitive energetic plasticiser containing nitrate ester and nitramine groups, is characterised by a good plastic dissolution effect for nitrocellulose (NC) [5], a low melting point [6] and low volatility [7]. The low melting point is beneficial with regard to improvement in the cryogenic mechanical properties of the propellant; at the same time, the volatility of a blend of BuNENA and NC is only half that of NG and NC. BuNENA can be introduced into the formulation of NC-based propellants, glycidyl azide polymer (GAP)-based propellants, and hydroxy-terminated polyether (HTPE)-based propellants as an insensitive plasticiser [8, 9].

In order to introduce BuNENA into the formulation of a XLDB propellant, BuNENA-modified NC microspheres (BMNM) had to be prepared. Spherical powders form an important component of XLDB propellants. The theory of preparing a spherical powder using the internal dissolution method was proposed by Olsen in 1936 [10]. The internal dissolution method, also called the solvent evaporation method, has the advantages of using simple equipment and being a mature technology. However, owing to some of the stabilisers and emulsifiers being utilised during the granulation processes, the ingredients of such spherical powders are complicated and their particle size varies significantly. The present research involved the preparation of BuNENA-modified NC microspheres by the 'breath figures' method without using any additives. 'Breath figures' is the most simple, but effective, self-assembly method, and was first investigated by Lord Rayleigh in 1911 [11]. Using this method, Francois *et al*. made ordered, porous, polymer films in 1994 [12] and investigated the films prepared by the 'breath figures' method thereafter [13-15]. In 2009, a polymer microsphere was obtained for the first time by Xiong *et al.*, by changing the atmosphere in which the specimen was prepared from water to an organic solvent, methanol [16]. NC microspheres and BuNENA modified NC microspheres (BMNM) were prepared using the 'breath figures' method in this research. The work should provide a new preparative method for spherical powders.

2 Experimental

2.1 Materials and instruments

Materials: BuNENA, a light yellow liquid, was purchased from the Liming Research Institute of Chemical Industries, Luoyang; Grade D nitrocellulose was

Copyright © 2016 Institute of Industrial Organic Chemistry, Poland

purchased from Luzhou North Chemical Industry Co. Ltd, Luzhou; acetone, tetrahydrofuran, ethyl acetate, and n-hexane were analytically pure and purchased from Xilong Chemical Industry Co. Ltd.

Instruments: a DSC1 differential scanning calorimeter and a TGA1 thermogravimetric analyser produced by Mettler Toledo, Switzerland, and a three-dimensional microscope system (VHX-2000, Keyence, Japan) were used.

2.2 Sample preparation

An acetone solution containing the NC was prepared by dissolving the NC in acetone to a concentration of 5 mg/mL. A holder was placed in a beaker (50 mL) with a sealing cover and the non-solvent (5 mL; for example, methanol, n-hexane, *etc.*) was added at room temperature to provide the necessary atmosphere for the preparation. The upper surface of the holder above the level of the liquid and a cleaned glass slide (1 cm × 1 cm) was placed on the holder in the beaker. The beaker was then sealed for a few minutes to saturate the atmosphere. Afterwards, the polymer solution (5 μL) was dropped rapidly onto the surface of the glass slide using a micro-injector. After the solvent (acetone) had evaporated (and thereafter), the glass slide was removed and NC microspheres were obtained.

A solution was prepared by adding NC (70 mg) and BuNENA (30 mg) to acetone (20 mL); the BMNM were acquired in the same way as the NC microspheres. The process, in the non-solvent vapour atmosphere, is shown in Figure 1.

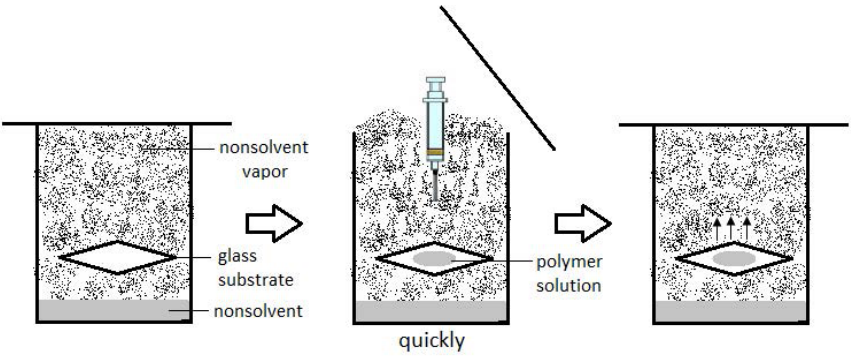

Figure 1. Microsphere manufacturing process.

2.3 Measurements

A three-dimensional microscope system was used to observe the morphologies of the microspheres. Besides this, a DSC1 differential scanning calorimeter and a TGA1 thermogravimetric analyser were used to investigate the thermal

Copyright © 2016 Institute of Industrial Organic Chemistry, Poland

decomposition kinetics of the microspheres. The sample holder was an aluminium crucible for the DSC analysis, and an Al_2O_3 crucible for the TG analysis (at applied heating rates of 5, 10, 15, and 20 K/min).

3 Results and Discussion

3.1 Influence of different atmospheres on the final morphology of the NC

Non-solvents for NC, n-hexane and water, were used as the atmosphere, while acetone and tetrahydrofuran were favourable solvents. The 'breath figures' method was adopted to investigate the influence of different solvents and atmospheres on the final morphology of the NC.

Figure 2(a-c) shows the final morphologies formed with different solvents in various atmospheres as observed by the optical microscope (OM). Microspheres could be obtained with solvents acetone and tetrahydrofuran, and an atmosphere of n-hexane, giving a particle size of less than 1 μm. The microspheres which were obtained using tetrahydrofuran as the solvent adhered to each other, while those obtained using acetone showed better dispersity. Porous films could be acquired if water was used as the atmosphere. This situation might have been caused by the differences in surface tension between n-hexane and water.

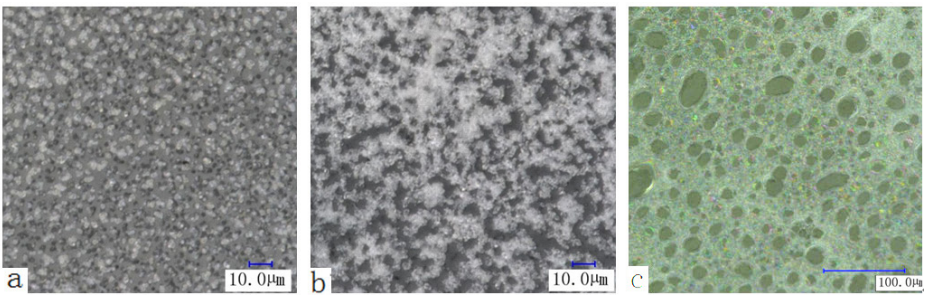

Figure 2. OM images of NC microspheres prepared in different solvent/non-solvent systems: (a) acetone/n-hexane , (b) tetrahydrofuran/n-hexane, (c) acetone/water

The surface tension of n-hexane is smaller than that of the polymer solution, therefore, when n-hexane was used as the atmosphere, the local concentration of the polymer solution increased and spheres were formed due to the surface tension effect. In the presence of water, as the water droplets, with their high

Copyright © 2016 Institute of Industrial Organic Chemistry, Poland

surface tension, spread over the polymer solution, porous films were formed after evaporation of the solvent.

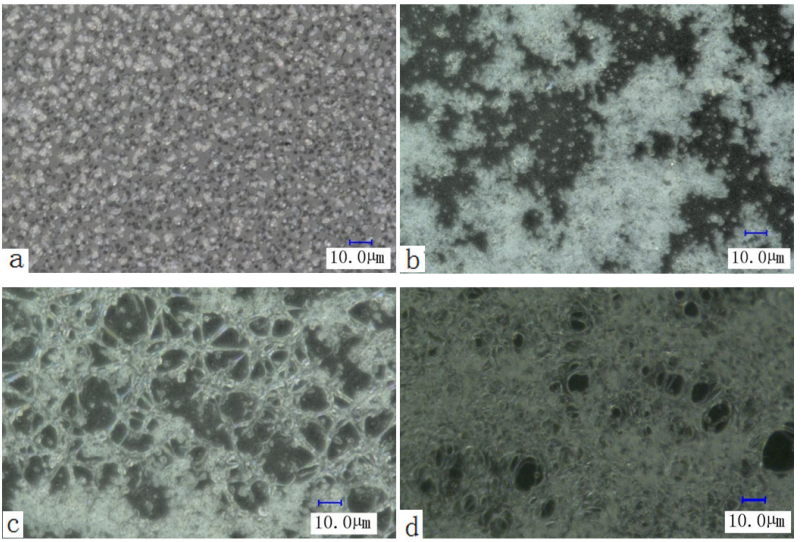

Figure 3. OM images of NC microspheres prepared from solutions of different concentrations: (a) 5 mg/mL, (b) 10 mg/mL, (c) 15 mg/mL, (d) 20 mg/mL.

Figure 3(a-d) shows optical micrographs of the final morphology of NC from acetone solutions at different concentrations, in a cyclohexane atmosphere: the NC solution with a concentration of 5 mg/mL formed uniformly scattered microspheres, while at 10 mg/mL and 15 mg/mL, the microspheres became clustered together. Some polymers formed a network-like morphology, with clustered microspheres inside. Moreover, when the concentration of the NC solution was increased to 20 mg/mL, the microspheres were glued together and formed films with uneven pores (both in size and distribution). This was because, when the concentration of the polymer solution was low, the polymer macromolecules became distributed in the solvent without intertwining. As the solvent evaporated, they rolled up into microspheres. By contrast, when the concentration of the solution was increased, the number of macromolecules in the solvent also increased so that some macromolecules intertwined with each other and then formed the observed network-like morphology during self-assembly. With increasing solution concentration, most macromolecules intertwined to form polymer films. Thus, the concentration of the polymer exerted a significant influence on the final morphology.

Copyright © 2016 Institute of Industrial Organic Chemistry, Poland

The morphology of the BMNM microspheres obtained by adding BuNENA to the acetone solution of NC is shown in Figure 4; the microspheres were better dispersed.

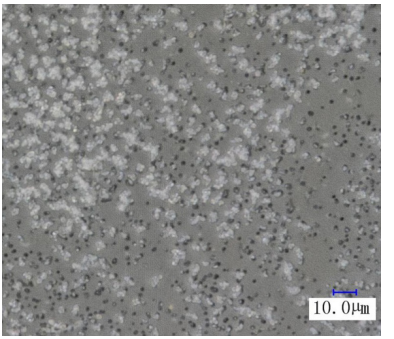

Figure 4. OM image of BMNM prepared in an acetone/n-hexane system.

There are several views as to whether, or not, the final morphology obtained by the 'breath figures' method is microspherical or akin to a porous film. Xiong [16] considered that the morphology of a polymer (either microspherical or as a porous film) after assembly mainly depended on the differences in surface tension between the polymer solution and the non-solvent. In general, if the difference was positive and higher than 1.5 mN/m, microspheres were obtained, otherwise, porous films were produced. Huang [17] believed that the surface tension is not the major factor governing the morphology of the microspheres or porous membranes. On the contrary, the interaction between solvents and non-solvents and the polymer is likely to influence the morphology after polymer assembly. In other words, the morphology of the polymer is affected by many factors. Bai [18] found that the interaction between the droplets and the solution is the key process behind the creation of different patterns. Combining the experimental results and evidence from the available literature, it was found that the morphology of the polymer was generally microspherical when the difference in surface tension between the polymer solution and its non-solvent was positive; however, this was a necessary, but not sufficient, condition with regard to its influence on the final morphology. In addition, the final morphology was also affected by factors such as the concentration of the solution, polarity, the saturated vapour pressure of the solvents, and the non-solvents, *etc*. Hence, the key factors influencing the final morphology were the appropriate concentration of the solution and the matching of solvents and non-solvents. Table 1 summarises the literature on the solvent matching conditions needed to form microspheres.

Copyright © 2016 Institute of Industrial Organic Chemistry, Poland

Table 1. Examples of microsphere patterns: solvent and non-solvent

Solvent	Non-solvent	Reference(s)
Acetone	n-Hexane	-
Tetrahydrofuran	n-Hexane	-
Toluene	Ethanol	16
Toluene	Methanol	16
Chloroform	Methanol	16, 17
Chloroform	Ethanol	17
Chloroform	n-Hexane	17
Dichloromethane	Methanol	16, 18

3.2 Thermal decomposition of BMNM

To explore the influence on the thermal decomposition performance of the composite granulation of NC and BuNENA, thermogravimetry (TG) and differential scanning calorimetry (DSC) were performed for BMNM with 30% BuNENA, and NC microspheres. The TG curves at a heating rate of 5 K/min are shown in Figure 5.

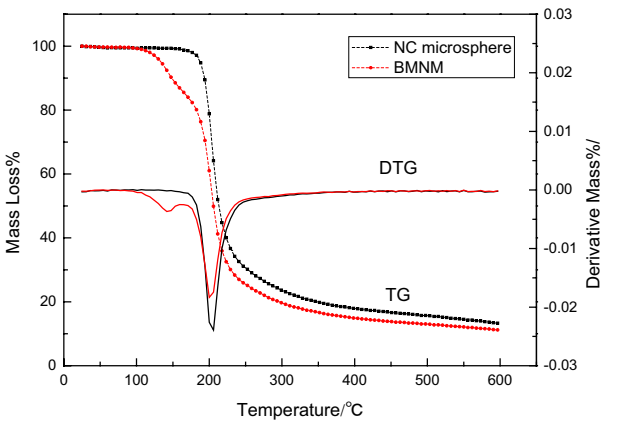

Figure 5. TG curves of BMNM and NC microspheres.

The TG curve of BMNM showed two distinct mass loss regions as the temperature increased from 30 °C to 600 °C. The first region was the mass loss (13.8%) associated with volatilisation of BuNENA in the temperature range 101.6 °C to 165.6 °C. The peak temperature seen on the DTG curve was 143.2 °C. The second region was aligned with the thermal decomposition of NC and the residual BuNENA in the temperature range 167 °C to 600 °C; the peak temperature seen on the DTG curves was 201.8 °C. The second region

Copyright © 2016 Institute of Industrial Organic Chemistry, Poland

was divided into two consecutive decomposition processes. In the first process (166.76 °C to 251.4 °C) the mass loss was 59.89%, and 13.96% in the second process (252.6 °C to 600 °C). The temperature range was consistent with that of the decomposition of NC microspheres and confirmed that the thermal decomposition process of NC was not changed by the addition of BuNENA.

The decomposition of nitrate esters falls into three categories: domination of the decomposition product of side chain nitrate esters, competition between the decomposition products of nitrate and the framework, and the domination of the decomposition product of the framework [19]. Both BuNENA and NC belong to the second category of nitrate esters. NC is considered as the second kind of nitrate ester, which means that a large amount of NO_2 produced by the rupture of the nitrate ester bond remains in the framework of the polymer to enhance the second-order autocatalytic reaction. The condensed phase reaction dominates the entire reaction process. The BuNENA in BMNM was uniformly distributed among the NC macromolecules. Upon heating, the nitrate ester base of BuNENA, and that of NC, would decompose at the same time, while the NO_2 produced by subsequent ruptures was stranded in the condensed phase to further affect the autocatalytic decomposition in the framework of the polymer, so as to accelerate the pyrolysis of the framework of NC and BuNENA.

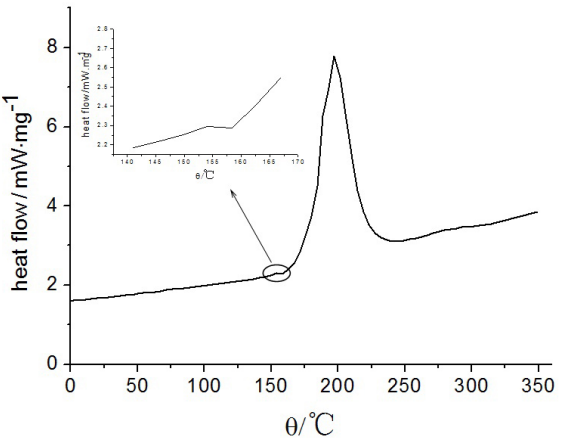

Figure 6. DSC curve of BMNM.

Figure 6 shows the DSC curve of BMNM at a heating rate of 5 K/min. The first small endothermic peak was observed at 160 °C, and corresponded to the first mass loss region of the TG curve, namely, that arising from the volatilisation of BuNENA. The exothermic peak appeared at 200 °C and corresponded to the

Copyright © 2016 Institute of Industrial Organic Chemistry, Poland

second mass loss phase of the TG curve, namely, the decomposition and heat release of NC and the residual BuNENA.

To understand the thermal decomposition characteristics of BMNM more intuitively, the Kissinger method [20-22] (see Equation 1) and the Ozawa method [23, 24] (see Equation 2) were applied to calculate the activation energies of NC microspheres and BMNM in the thermal mass loss phases.

$$\ln\left(\frac{\beta}{T^2}\right) = \ln\left(\frac{AR}{E_a}\right) - \frac{E_a}{RT} \tag{1}$$

$$\lg\beta = \ln\frac{AE_a}{G(\alpha)R} - 2.351 - 0.4567\frac{E_a}{RT} \tag{2}$$

where, T is the absolute thermodynamic temperature (K); α is the reaction rate at T; A is a pre-exponential factor; R is the ideal gas constant; E_a is the activation energy; and $G(\alpha)$ is the reaction mechanism function. In the Kissinger equation, X and Y are $\frac{1}{RT}$ and $\ln\left(\frac{\beta}{T^2}\right)$ respectively, while X and Y are $\frac{0.4567}{RT}$ and $\lg\beta$ respectively in the Ozawa equation. The standard deviation was calculated using the STDEV function in Excel and the standard error of estimate was calculated using the STEYX function in Excel. These values are listed in Tables 2 and 3.

Table 2. Determination of the activation energies for the degradation of BMNM by the Kissinger method

	α	E_a [kJ/mol]	ln(A) [s^{-1}]	S_X	S_Y	Standard error of estimate
BMNM	5 to 20	68.54	14.29	7.91E-06	0.5448	0.0591
BMNM	20 to 70	249.53	51.81	2.32 E-06	0.5827	0.0667
NC microsphere	5 to 65	253.45	59.70	2.29 E-06	0.5828	0.0154

Note: S_X is the standard deviation of the X values; S_Y is the standard deviation of the Y values.

The similar activation energy values computed by the two methods are listed in Tables 2 and 3. The results show that the thermal mass loss of BMNM included two stages: the first corresponded to the volatilisation of BuNENA with its low activation energy, the value calculated by use of the Kissinger method being 68.54 kJ/mol. Corresponding to the thermal decomposition of NC, the activation energy of the second phase was higher, with a value of 249.53 kJ/mol by the Kissinger method, which is close to that for the NC microspheres, 253.45 kJ/mol. This also illustrated that the addition of BuNENA did not change the thermal decomposition of NC in the spherical powder.

Copyright © 2016 Institute of Industrial Organic Chemistry, Poland

Table 3. Determination of the activation energies for the degradation of BMNM by the Ozawa method

	α	E_a [kJ/mol]	S_X	S_Y	Standard error of estimate
BMNM	5 to 20	71.98	3.61 E-06	0.2611	0.0254
BMNM	20 to 70	244.89	1.06 E-06	0.2611	0.0289
NC microsphere	5 to 65	248.60	1.05 E-06	0.2611	0.0066

Note: S_X is the standard deviation of the X values; S_Y is the standard deviation of the Y values.

To describe the thermal decomposition mechanism of BMNM, model fitting to the TG curve of BMNM was carried out by the Coats-Redfern method [25] (see Equation 3).

$$\ln\left[\frac{G(\alpha)}{T^2}\right] = \ln\left[\frac{AR}{\beta E}\left(1-\frac{2RT}{E}\right)\right] - \frac{E}{RT} \tag{3}$$

where, T is the absolute thermodynamic temperature (K); α is the reaction rate at T; A is a pre-exponential factor; R is the ideal gas constant; E is the activation energy; and $G(\alpha)$ is the reaction mechanism function. In terms of the general reaction temperature, and most E values, $2RT/E << 1$, so is almost constant. The values of E and A can be found from the slope of the linear regression relationship of $\ln[G(\alpha)/T^2]$—$1/T$. The parameters, including the activation energy, the pre-exponential factor, and the correlation coefficient can be obtained by substituting the experimental data into the corresponding equations for the 15 types of common mechanism functions. The mechanism function which gives the largest correlation coefficient and an activation energy value which most closely approximates to the value obtained by the Ozawa method, can be deemed to be the most probable mechanism function. By substituting the experimental data into the corresponding equation of the commonly used mechanism function, the thermal decomposition kinetics model (see Table 4) was established. The results indicated that the optimal kinetics models for NC microspheres and BMNM were A2 and B1-A2, respectively.

Table 4. Optimised kinetics model and kinetic parameters for the degradation of BMNM

	α	Mecha-nism	$G(\boldsymbol{\alpha})$	E_a [kJ/mol]	$\ln(A)$ [s^{-1}]	Correlation coefficient
BMNM	5 to 20	B1	$\ln[\boldsymbol{\alpha}/(1-\boldsymbol{\alpha})]$	145.5	33.5	0.9971
BMNM	20 to 70	A2	$[-\ln(1-\boldsymbol{\alpha})]^{1/2}$	233.4	53.2	0.9939
NC microsphere	5 to 65	A2	$[-\ln(1-\boldsymbol{\alpha})]^{1/2}$	248.1	54.8	0.9755

Copyright © 2016 Institute of Industrial Organic Chemistry, Poland

4 Conclusions

The 'breath figures' method was used to prepare NC microspheres and BMNM. By adopting acetone as the solvent and n-hexane as the non-solvent atmosphere, NC microspheres and BMNM were obtained; porous films were obtained when water was used as the atmosphere. The matching of solvents and non-solvents was the key factor influencing the final morphology. When the concentration of the solution was low (*i.e*. between 5 and 10 mg/mL), it was more likely that microspheres would be produced rather than porous films, under conditions in which the solvent had the greater surface tension, and a similar, or smaller, saturated vapour pressure than those of the non-solvent.

TG and DSC analyses were applied to study the thermal decomposition characteristics of BMNM. The results suggested that there were two distinct stages of thermal mass loss from the BMNM: the first was the mass loss associated with part-volatilisation of BuNENA, with an activation energy was 68.54 kJ/mol; the second was the thermal decomposition of NC and residual BuNENA, with a high activation energy (249.53 kJ/mol, calculated using the Kissinger method). According to the thermal decomposition kinetics model, the optimal kinetics model of BMNM was B1-A2. The addition of BuNENA did not influence the thermal decomposition of NC.

References

[1] Kumari D., Balakshe R., Banerjee S., Singh H., Energetic Plasticizers for Gun and Rocket Propellant, *Rev. J. Chem.*, **2012**, *2*(3), 240-262.
[2] Damse R.S., Omprakash B., Tope B.G., Chakraborthy T.K., Singh A., Study of N-n-butyl-N-(2-nitroxyethyl)nitramine in RDX Based Gun Propellant, *J. Hazard. Mater.*, **2009**, *167*(1), 1222-1225.
[3] Min B.S., Park Y.C., A Study on the Aliphatic Energetic Plasticizers Containing Nitrate Ester and Nitramine, *J. Ind. Eng. Chem.*, **2009**, *15*(4), 595-601.
[4] Türker L., Atalar T., Computational Studies on Nitratoethylnitramine (NENA) its Tautomers and Charged Forms, *J. Hazard. Mater*., **2009**, *162*(1), 193-203.
[5] Qi X., Zhang X., Guo X., Zhang W., Chen Z., Zhang J., Experiments and Simulation on Plastication of NENA on NC, *J. Solid Rocket Technol.* (*Guti Huojian Jishu*), **2013**, *36*(4), 516-520.
[6] Urenovitch J.V., *Low Vulnerability Propellant Plasticizers*, Patent US 5482581, **1996**.
[7] Cartwright R.V., Volatility of NENA and Other Energetic Plasticizers Determined Thermogravimetric Analysis, *Propellants Explos. Pyrotech.*, **1995**, *20*(2), 51-57.
[8] Landsem E., Jensen T.L., Hansen F.K., Unneberg E., Kristensen T.E., Neutral

Copyright © 2016 Institute of Industrial Organic Chemistry, Poland

Polymeric Bonding Agents (NPBA) and Their Use in Smokeless Composite Rocket Propellants Based on HMX-GAP-BuNENA, *Propellants Explos. Pyrotech.*, **2012**, *37*(5), 581-591.

[9] Gholamian M.A.F., Zarei A.R., Noncrystalline Binder Based Composite Propellant, *ISRN Aerospace Engineering*, **2013**; doi:10.1155/2013/679710.

[10] Fredrich O., Tibbitts G.C., Kerone E.B.W., *Manufacture of Smokeless Powders*, Patent US 2027114, **1936**.

[11] Rayleigh L, Breath Figures, *Nature*, **1911**, *86*(2169), 416-417.

[12] Widawski G., Rawiso M., François B., Self-organized Honeycomb Morphology of Star-polymer Polystyrene Films, *Nature*, **1994**, *369*, 387-389.

[13] Ferrari E., Fabbri P., Pilati F., Solvent and Substrate Contributions to the Formation of Breath Figure Patterns in Polystyrene Films, *Langmuir*, **2011**, *27*(5), 1874-1881.

[14] Ucar I.O., Erbil H.Y., Dropwise Condensation Rate of Water Breath Figures on Polymer Surfaces Having Similar Surface Free Energies, *Appl. Phys. Lett*., **2012**, *259*, 515-23.

[15] Huh M., Jung M.H., Park Y.S., Kang T.B., Nah C., Russell R.A., Holden P.J., Yun S.I., Fabrication of Honeycomb-structured Porous Films from Poly(3-hydroxybutyrate) and Poly(3-hydroxybutyrate-co-3-hydroxyvalerate) via the Breath Figures Method, *Polym. Eng. Sci.*, **2012**, *52*(4), 920-926.

[16] Xiong X., Zou W., Yu Z., Duan J., Liu X., Fan S., Zhou H., Microsphere Pattern Prepared by a "Reverse" Breath Figure Method, *Macromolecules*, **2009**, *42*(23), 9351-9356.

[17] Huang C.M., Zhang M., Wang D.H., Bai W.B., Xu Y.L., Lin J.H., Fabrication of Polymeric Microspheres by Breath Figures in Different Nonsolvent Atmospheres, *Acta Polymerica Sinica*, **2014**, *12*, 1606-1612.

[18] Bai W., Xiao X., Cai L., Fabrication of Morphology-controlled Nano/Microstructural Polyfluorene in Mixed Nonsolvent Vapor Atmospheres, *React. Funct. Polym.*, **2014**, *76*, 13-18.

[19] Oyumi Y., Brill T.B., Thermal Decomposition of Energetic Materials. 14. Selective Product Distributions Evidenced in Rapid, Real-time Thermolysis of Nitrate Esters at Various Pressures, *Combust. Flame*, **1986**, *66*(1), 9-16.

[20] Kissinger H.E., Reaction Kinetics in Differential Thermal Analysis, *Anal. Chem.*, **1957**, *29*(11), 1702-1706.

[21] Kissinger H.E., Variation of Peak Temperature with Heating Rate, *J. Res. Natl. Bur. Stand.*, **1956**, *57*(4), 217-222.

[22] Hu R.Z., Shi Q.Z., *Kinetics of Thermal Analysis* (in Chinese), Science Press, Beijing, **2001**, pp. 65-66; ISBN 7-03-00946-3/O.1511.

[23] Ozawa T., A Modified Method for Kinetic Analysis of Thermoanalytical Data, *J. Therm. Anal. Calorim.*, **1976**, *9*(3), 369-373.

[24] Zhan D., Cong C., Diakite K., Tao Y., Zhang K., Kinetics of Thermal Decomposition of Nickel Oxalate Dihydrate in Air, *Thermochim. Acta*, **2005**, *430*(1), 101-105.

[25] Coats A.W., Redfern J.P., Kinetic Parameters from Thermogravimetric Data, *Nature*, **1964**, *201*, 68-69.

Copyright © 2016 Institute of Industrial Organic Chemistry, Poland